Partial-wave analysis of nucleon-nucleon scattering below the pion-production threshold

R. Navarro Pérez,* J. E. Amaro,† and E. Ruiz Arriola‡
Departamento de Física Atómica, Molecular y Nuclear and Instituto Carlos I de Física Teórica y Computacional, Universidad de Granada, E-18071 Granada, Spain
(Received 12 April 2013; revised manuscript received 27 June 2013; published 5 August 2013)

We undertake a simultaneous partial wave analysis of proton-proton and neutron-proton scattering data below the pion production threshold up to laboratory energies of 350 MeV. We represent the interaction as a sum of δ shells in configuration space below 3 fm and a charge dependent one pion exchange potential above 3 fm together with electromagnetic effects. We obtain a chi square value of 2813, for *pp*, and 3985, for *nn*, with a total of 2747 and 3691 *pp* and *nn* data, respectively, obtained till 2013 and a total number of 46 fitting parameters yielding a chi square value by degree of freedom of $\chi^2/\text{d.o.f} = 1.06$. Special attention is payed to estimate the errors of the phenomenological interaction as well as the derived effects on the phase shifts and scattering amplitudes.

DOI: 10.1103/PhysRevC.88.024002 PACS number(s): 03.65.Nk, 11.10.Gh, 13.75.Cs, 21.30.Fe

I. INTRODUCTION

The nucleon-nucleon (NN) interaction plays a central role in nuclear physics (see, e.g., [1,2] and references therein). The standard procedure to constrain the interaction uses a partial wave analysis (PWA) of the proton-proton (pp) and neutron-proton (np) scattering data below the pion production threshold [3] although there are accurate descriptions up to 3 GeV for pp and 1.3 GeV for np [4]. The Nijmegen PWA uses a large body of NN scattering data yielding a chi square value by degree of freedom $\chi^2/\text{d.o.f} \lesssim 1$ after discarding about 20% of 3σ inconsistent data, where σ is the standard deviation [5] (see, however, [4] where $\chi^2/\text{d.o.f} = 1.4$ without the 3σ criterium). This fit incorporates charge dependence (CD) for the one pion exchange (OPE) potential as well as electromagnetic, vacuum polarization and relativistic effects, the latter being key ingredients to this accurate success. The analysis was more conveniently carried out using an energy dependent potential for the short range part. Later on, energy independent *high quality* potentials were designed with almost identical $\chi^2/\text{d.o.f} \sim 1$ for the gradually increasing database [6–9]. While any of these potentials provides individually satisfactory fits to the available experimental data, an error analysis would add a means of estimating quantitatively the impact of NN-scattering uncertainties in nuclear structure calculations. In the present paper we provide a high-quality potential implementing an analysis of its parameter uncertainties using the standard method of inverting the covariance matrix [10].

The paper is organized as follows. In Sec. II we briefly review the main aspects of the formalism. After that, in Sec. III we present our numerical results and fits as well as our predictions for deuteron properties and scattering amplitudes. Finally, in Sec. IV we summarize our results and come to the conclusions.

*rnavarrop@ugr.es
†amaro@ugr.es
‡earriola@ugr.es

II. FORMALISM

The complete on-shell NN scattering amplitude contains five independent complex quantities, which we choose for definiteness as the Wolfenstein parameters [3],

$$M(\mathbf{k}_f, \mathbf{k}_i) = a + m(\sigma_1, \mathbf{n})(\sigma_2, \mathbf{n}) + (g - h)(\sigma_1, \mathbf{m})(\sigma_2, \mathbf{m}) + (g + h)(\sigma_1, \mathbf{l})(\sigma_2, \mathbf{l}) + c(\sigma_1 + \sigma_2, \mathbf{n}), \quad (1)$$

where a, m, g, h, c depend on energy and angle; σ_1 and σ_2 are the single nucleon Pauli matrices; $\mathbf{l}$, $\mathbf{m}$, $\mathbf{n}$ are three unitary orthogonal vectors along the directions of $\mathbf{k}_f + \mathbf{k}_i$, $\mathbf{k}_f - \mathbf{k}_i$, and $\mathbf{k}_i \wedge \mathbf{k}_f$; and $\mathbf{k}_f, \mathbf{k}_i$ are the final and initial relative nucleon momenta, respectively. To determine these parameters and their uncertainties we find that a convenient representation to sample the short distance contributions to the NN interaction can be written as a sum of δ shells:

$$V(r) = \sum_{n=1}^{18} O_n \left[\sum_{i=1}^{N} V_{i,n} \Delta r_i \delta(r - r_i) \right] + [V_{\text{OPE}}(r) + V_{\text{em}}(r)]\theta(r - r_c), \quad (2)$$

where O_n are the set of operators in the AV18 basis [7], $r_i \leqslant r_c$ are a discrete set of N radii, and $\Delta r_i = r_{i+1} - r_i$ and $V_{i,n}$ are unknown coefficients to be determined from the data. The $V_{OPE}(r)$ and $V_{em}(r)$ functions in the $r > r_c$ piece are the CD OPE potential and the electromagnetic (EM) correction, respectively, which are kept fixed throughout. The solution of the corresponding Schrödinger equation in the (coupled) partial waves $^{2S+1}L_J$ for $r \leqslant r_c$ is straightforward since the potential reads

$$V^{JS}_{l,l'}(r) = \frac{1}{2\mu_{\alpha\beta}} \sum_{i=1}^{N} (\lambda_i)^{JS}_{l,l'} \delta(r - r_i) \quad r \leqslant r_c, \quad (3)$$

with $\mu_{\alpha\beta} = M_\alpha M_\beta/(M_\alpha + M_\beta)$ the reduced mass with $\alpha, \beta = n, p$. Here, $(\lambda_i)^{JS}_{l,l'}$ are related to the $V_{i,n}$ coefficients by a linear transformation at each discrete radius r_i. Thus, for any $r_i < r < r_{i+1}$ we have free particle solutions, and log-derivatives are discontinuous at the r_i radii so that one generates an accumulated S matrix at any sampling radius providing a discrete and purely algebraic version of Calogero's variable phase equation [17].

This form of potential effectively implements a coarse graining of the interaction, first proposed 40 years ago by Aviles [18]. We have found that the representation (3) is extremely convenient and computationally cheap for our PWA. The low energy expansion of the discrete variable phase equations was used already in Ref. [19] to determine threshold parameters in all partial waves. The relation to the well-known Nyquist theorem of sampling a signal with a given bandwidth has been discussed in Ref. [20]. Some of the advantages of directly using this simple potential for nuclear structure calculations have also been analyzed [21].

The fact that we are coarse graining the interaction enables us to encode efficiently all effects operating below the finest resolution Δr which we identify with the shortest de Broglie wavelength corresponding to the pion production threshold, $\lambda_{\min} \sim 1/\sqrt{m_\pi M_N} \sim 0.55$ fm, so that a maximal number of δ shells $N = r_c/\Delta r \sim 5$ (for $r_c = 3$ fm) should be needed. In practice, we expect the number of sampling radii to decrease with angular momentum as the centrifugal barrier makes irrelevant those radii $r_i \lesssim (l + 1/2)/p$ below the relevant impact parameter, so that the total number of δ shells and hence fitting strengths $V_{i,n}$ will be limited and smaller than $N = 5$.

The previous discretization of the potential is just a way to numerically solve the Schrödinger equation for any given potential where one replaces $V(r) \to \bar{V}(r) = \sum_i V(r_i)\Delta r_i \delta(r - r_i)$, but the number of δ shells may be quite large for *fixed* strengths $V_i \equiv V(r_i)$. For instance, for the $^1S_0$ wave and for the AV18 [7] potential one needs $N = 600\delta$ shells to reproduce the phase shift with sufficient accuracy (below 10^{-4} degrees) but just $N = 5$ if one uses $V(r_i)$ as fitting parameters to the *same* phase shift [21].

The EM part of the NN potential gives a contribution to the scattering amplitude that must be taken into account properly in order to correctly calculate the different observables. Each term of the electromagnetic potential in the pp and np channels needs to be treated differently to obtain the corresponding parts of the total EM amplitude. The expressions for the contributions coming from the pp one photon exchange potential V_{C1}, and the corresponding relativistic correction V_{C2}, are well known and can be found in [5]. To calculate the contribution of the vacuum polarization term V_{VP} we used the approximation to the amplitude given in [22]. Finally, Ref. [23] details the treatment of the magnetic moment interaction V_{MM} for both pp and np channels and the necessary corrections to the nuclear amplitude coming from the electromagnetic phase shifts.

III. NUMERICAL RESULTS

A. Coarse graining EM interactions

Of course, once we admit that the interaction below r_c is unknown there is no gain in directly extending the well-known charge-dependent OPE tail for $r \leqslant r_c$. Unlike the purely strong piece of the NN potential the electromagnetic contributions are known with much higher accuracy and to shorter distances (see, e.g., Ref. [7]) so that one might extend $V_{\rm em}(r)$ below r_c adding a continuous contribution on top of the δ shells, so that the advantage of having a few radii in the region $r \leqslant r_c$ would be lost. To improve on this we coarse grain the EM interaction up to the pion production threshold. Thus, we look for a discrete representation on the grid of the purely EM contribution $V_{\rm em}(r)$, i.e., we take $\bar{V}_{\rm em}(r) = \sum_n V_i^C \Delta r_i \delta(r - r_i) + \theta(r - r_c)V_{\rm em}(r)$, where the V_i^C are determined by reproducing the purely EM scattering amplitude to high precision and are not changed in the fitting process. The result using the EM potential of Ref. [7] just turns out to involve the Coulomb contribution in the central channel and the corresponding δ shell parameters $\lambda_i^C = V_i^C \Delta r_i M_p$

TABLE I. Fitting δ shell parameters $(\lambda_n)^{JS}_{l,l'}$ (in fm^{-1}) with their errors for all states in the JS channel. We take $N = 5$ equidistant points with $\Delta r = 0.6$ fm. The symbol "–" indicates that the corresponding fitting $(\lambda_n)^{JS}_{l,l'} = 0$. In the first line we provide the central component of the δ shells corresponding to the EM effects below $r_c = 3$ fm. These parameters remain fixed within the fitting process.

Wave	λ_1 ($r_1 = 0.6$ fm)	λ_2 ($r_2 = 1.2$ fm)	λ_3 ($r_3 = 1.8$ fm)	λ_4 ($r_4 = 2.4$ fm)	λ_5 ($r_5 = 3.0$ fm)
$V_C[pp]_{\rm EM}$	0.02091441	0.01816750	0.00952244	0.01052224	0.00263887
$^1S_0[np]$	1.28(7)	−0.78(2)	−0.16(1)	–	−0.025(1)
$^1S_0[pp]$	1.31(2)	−0.723(4)	−0.187(2)	–	−0.0214(3)
$^3P_0$	–	1.00(2)	−0.339(7)	−0.054(3)	−0.025(1)
$^1P_1$	–	1.19(2)	–	0.076(2)	–
$^3P_1$	–	1.361(5)	–	0.0579(5)	–
$^3S_1$	1.58(6)	−0.44(1)	–	−0.073(1)	–
ε_1	–	−1.65(1)	−0.34(2)	−0.233(8)	−0.020(3)
$^3D_1$	–	–	0.35(1)	0.104(9)	0.014(3)
$^1D_2$	–	−0.23(1)	−0.199(3)	–	−0.0195(2)
$^3D_2$	–	−1.06(4)	−0.14(2)	−0.243(6)	−0.019(2)
$^3P_2$	–	−0.483(1)	–	−0.0280(6)	−0.0041(3)
ε_2	–	0.28(2)	0.200(4)	0.046(2)	0.0138(5)
$^3F_2$	–	3.52(6)	−0.232(4)	–	−0.0139(6)
$^1F_3$	–	–	0.13(2)	0.091(8)	–
$^3D_3$	–	0.52(2)	–	–	–

TABLE II. Deuteron static properties compared with empirical values and high-quality potential calculations.

	δ shell	Empirical [11–16]	Nijm I [6]	Nijm II [6]	Reid93 [6]	AV18 [7]	CD-Bonn [8]
E_d (MeV)	Input	2.224575(9)	Input	Input	Input	Input	Input
η	0.02493(8)	0.0256(5)	0.02534	0.02521	0.02514	0.0250	0.0256
A_S (fm$^{1/2}$)	0.8829(4)	0.8781(44)	0.8841	0.8845	0.8853	0.8850	0.8846
r_m (fm)	1.9645(9)	1.953(3)	1.9666	1.9675	1.9686	1.967	1.966
Q_D (fm^2)	0.2679(9)	0.2859(3)	0.2719	0.2707	0.2703	0.270	0.270
P_D	5.62(5)	5.67(4)	5.664	5.635	5.699	5.76	4.85
$\langle r^{-1}\rangle$ (fm^{-1})	0.4540(5)			0.4502	0.4515		

are given in the first line of Table I. As expected from the Nyquist sampling theorem, we need at most $N = 5$ sampling points which for simplicity are taken to be equidistant with $\Delta r_i \equiv \Delta r = 0.6$ fm between the origin and $r_c = 3$ fm to coarse grain the EM interaction below $r \leqslant r_c$. Thus we should have $V_i^{pp} = V_i^{np} + V_i^C$ if charge symmetry was exact in strong interactions for $r < r_c$, although some corrections are expected as documented below.

B. Fitting procedure

In our fitting procedure we coarse grain the unknown short range part of the interaction from the scattering data. We use the $(\lambda_i)_{l,l'}^{JS}$'s as fitting parameters and minimize the value of the χ^2 using the Levenberg-Marquardt method where the Hessian is computed explicitly [24]. Actually, this is a virtue of our δ shell method which makes the computation of derivatives with respect to the fitting parameters analytical and straightforward. As a consequence, explicit knowledge of the Hessian allows for a faster search and finding of the minimum.

We start with a complete database compiling proton-proton and neutron-proton scattering data obtained till 2007 [25–27][1] and add two new data sets till 2013 [28,29]. We carry out at any rate a simultaneous pp and np fit for laboratory (LAB) kinetic energy below 350 MeV to published data only. Unfortunately, some groups of these data have a common but unknown normalization. We thus use the standard floating [30] by including an additional contribution to the χ^2 as explained in detail, e.g., in Ref. [9]. The extra normalization data are labeled by the subscript "norm" below. We also apply the Nijmegen PWA [5] 3σ criterion to reject possible outliers from the main fit with a 3σ-confidence level, a strategy reducing the minimal χ^2 but also enlarging the uncertainties. Initially we consider $N = 2717|_{pp,exp} + 151|_{pp,norm} + 4734|_{np,exp} + 262|_{np,norm} = 2868|_{pp} + 4996|_{np}$ fitting data and get $\chi^2_{\rm min} = 3310|_{pp} + 8518|_{np}$ yielding $\chi^2/{\rm d.o.f.} = 1.51$. Applying the 3σ rejection and refitting the remaining $N = 2747|_{pp} + 3691|_{np}$ data we finally obtain $\chi^2_{\rm min} = 2813|_{pp} + 3985|_{np}$ yielding a total $\chi^2/{\rm d.o.f} = 1.06$.

While the linear relations of the $(\lambda_i)_{l,l'}^{JS}$ and $V_{i,n}$ parameters are straightforward, limiting the number of operators O_n reduces the number of independent components of the potential in the different partial waves. The fitting parameters $(\lambda_n)_{l,l'}^{JS}$ entering the δ-shell potentials as independent variables, Eq. (3), are listed in Table I with their deduced uncertainties. All other partial waves are consistently obtained from those using the linear relations between $(\lambda_i)_{l,l'}^{JS}$ and $V_{i,n}$. Our final results allow us to fix the *same* pp and np potential parameters with the exception of the central components of the potential as it is usually the case in all joint $pp + np$ analyses carried out so far [5–8].

We find that introducing more points or equivalently reducing Δr generates unnecessary correlations and does not improve the fit. Also, lowering the value of r_c below 3 fm requires overlapping the short-distance potential, Eq. (3), with the OPE plus EM corrections. We find that independent fits to pp and np data, while reducing each of the χ^2 values, drive the minimum to incompatible parameters and erroneous np phases in isovector channels. Actually, the pp data constrain these channels most efficiently and in a first step pp fits where carried out to find suitable starting parameters for the corresponding np phases. Quite generally, we have checked that the minimum is robust by proposing several starting solutions.

As a numerical check of our construction of the amplitudes we reproduced the Wolfenstein parameters for the Reid93 and Nijm II potentials to high accuracy using $N = 12\,000$ δ-shell grid points, which ensures the correctness of the strong contributions. As a further check of our implementation of the long-range EM effects along the lines of Refs. [5,22,23] we have also computed the χ^2/d.o.f. for Reid93, Nijm II, and AV18 potentials (fitted to data prior to 1993) which globally and binwise are reasonably well reproduced when our database (coinciding with the one of Ref. [9] for np) includes only data prior to 1993.

C. Comparing with other database

In order to check the robustness of our database against other selections of data we take the current SAID world database [26] where unpublished data are also included and some further data have been deleted from their analysis although the total number exceeds our selected data. If we consider these $N_{\rm SAID} = 3061|_{pp,exp} + 188|_{pp,norm} + 4147|_{np,exp} + 411|_{np,norm} = 3249|_{pp} + 4558|_{np}$ data (without including their deleted data) we get for our main fit (without refitting) the value[2] $\chi^2/N_{\rm SAID} = 1.65$. Applying the 3σ

[1] The most recent np fit to these data was carried out in Ref. [9].

[2] We do not include 14 data of total pp cross section as our theoretical model includes all long range EM effects with no screening and, as is well known, the calculation diverges.

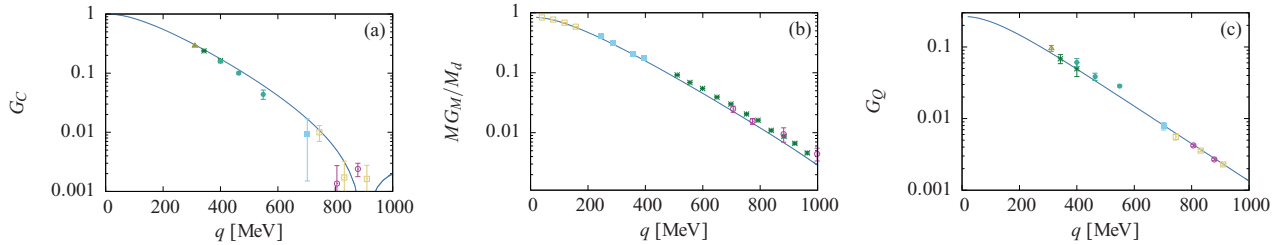

FIG. 1. (Color online) From left to right, charge, magnetic and quadrupole deuteron form factors, as a function of the momentum transfer, with theoretical error bands obtained by propagating the uncertainties of the $np + pp$ plus deuteron binding fit (see main text). Note that the theoretical error is so tiny that the width of the bands cannot be seen at the scale of the figure.

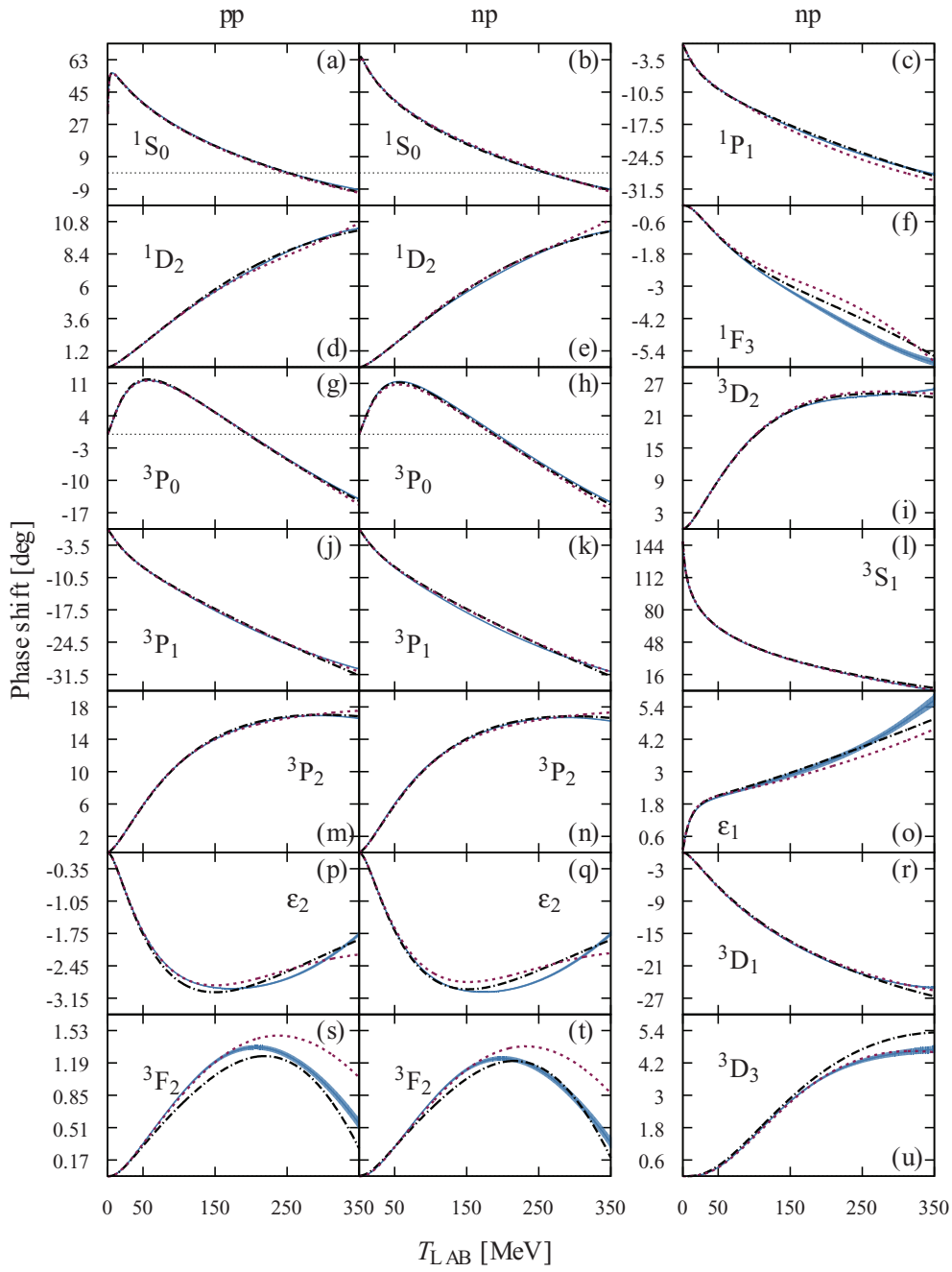

FIG. 2. (Color online) *np* and *pp* phase shifts and their propagated errors (blue band) corresponding to independent operator combinations of the fitted potential, as a function of the LAB kinetic energy. We compare our fit (blue band) with the PWA [5] (dotted, magenta) and the AV18 potential [7] (dashed-dotted, black) which gave χ^2/d.o.f $\lesssim 1$ for data before 1993.

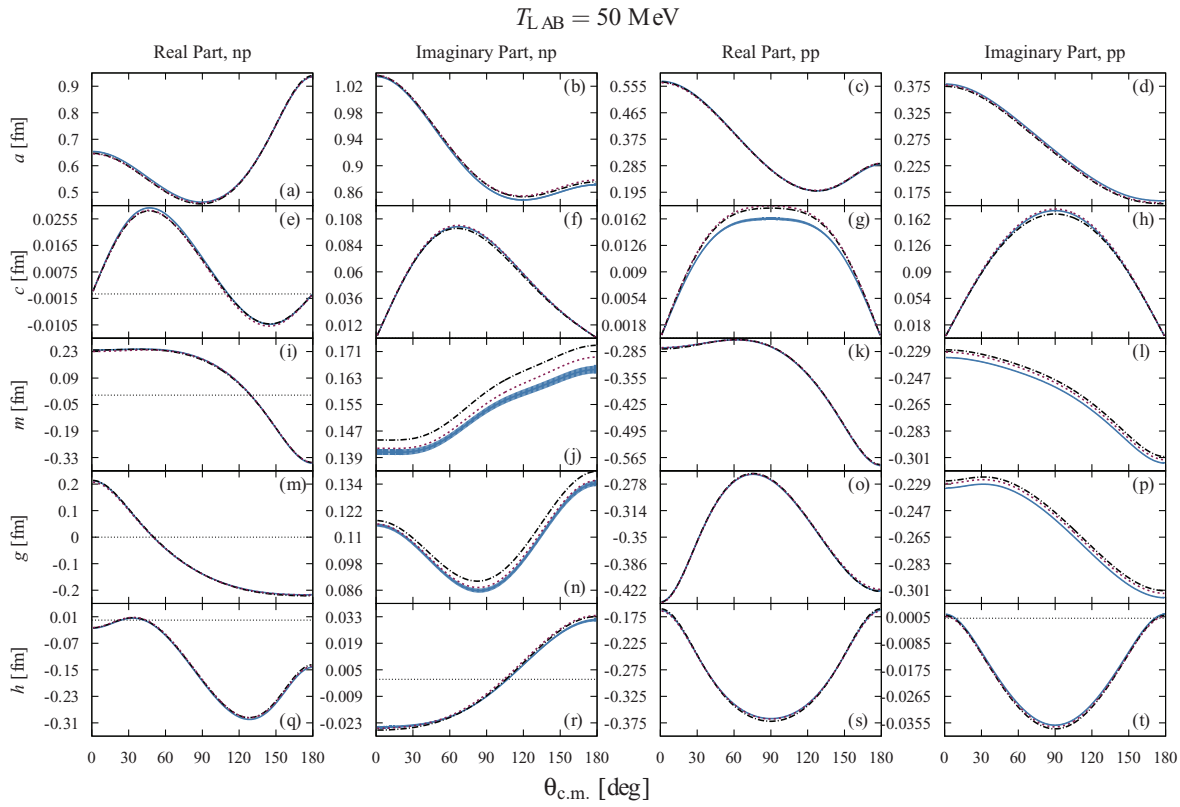

FIG. 3. (Color online) *np* (left) and *pp* (right) Wolfenstein parameters (in fm) as a function of the center of mass (CM) angle (in degrees) and for $E_{\mathrm{LAB}} = 50$ MeV. We compare our fit (blue band) with the PWA [5] (dotted, magenta) and the AV18 potential [7] (dashed-dotted, black) which provided a χ^2/d.o.f $\lesssim 1$ for data before 1993.

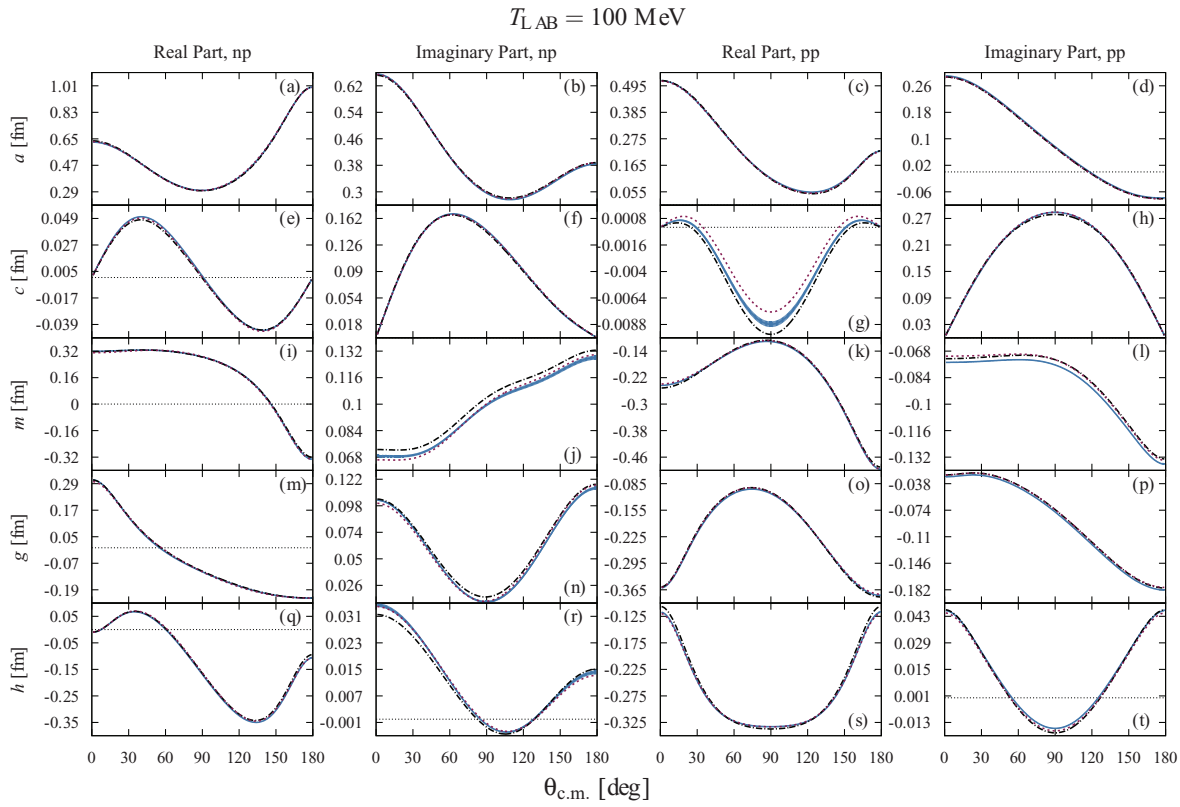

FIG. 4. (Color online) Same as in Fig. 3 but for $E_{\mathrm{LAB}} = 100$ MeV.

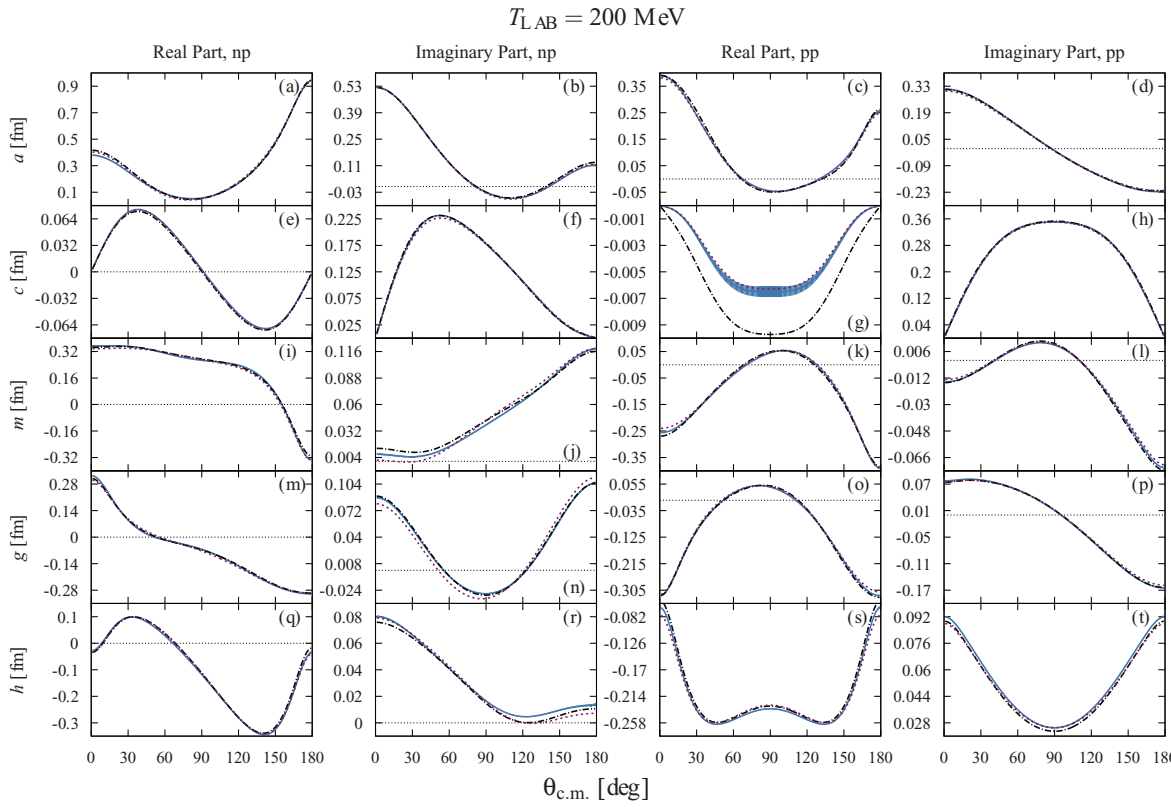

FIG. 5. (Color online) Same as in Fig. 3 but for $E_{\mathrm{LAB}} = 200$ MeV.

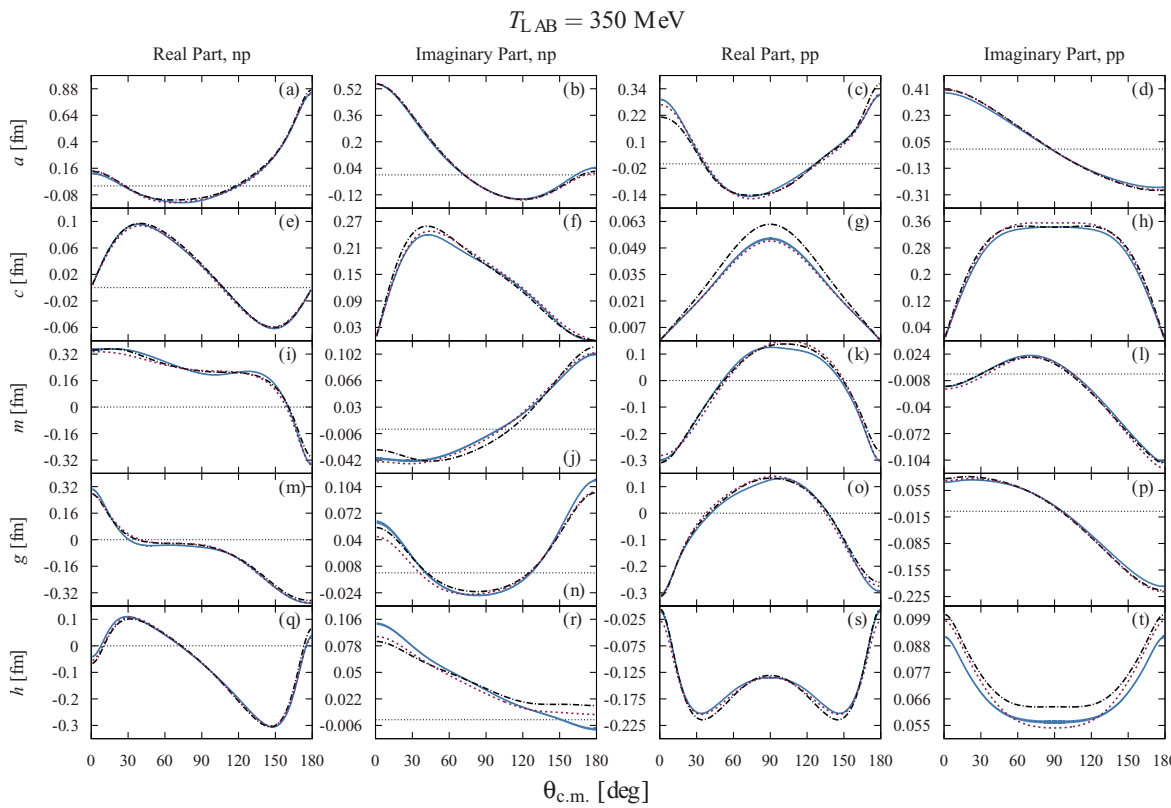

FIG. 6. (Color online) Same as in Fig. 3 but for $E_{\mathrm{LAB}} = 350$ MeV.

rejection to this database we get $\chi^2/N_{\rm SAID} = 1.04$. If instead we fit our model to this database we initially get $\chi^2/{\rm d.o.f.}|_{\rm SAID} = 1.31$ which after the 3σ selection of data becomes $\chi^2/{\rm d.o.f.}|_{\rm SAID} = 1.04$.

D. Error propagation

We determine the deuteron properties by solving the bound state problem in the ${}^3S_1 - {}^3D_1$ channel using the corresponding parameters listed in Table I. The predictions are presented in Table II where our quoted errors are obtained from propagating those of Table I by using the full covariance matrix among fitting parameters. The comparison with experimental values or high quality potentials where the deuteron binding energy is used as an input is satisfactory [5–9].

The outcoming and tiny theoretical error bands for the deuteron form factors (see, e.g., [31]) are depicted in Fig. 1 and are almost invisible at the scale of the figure. The rather small discrepancy between our theoretical results and experimental form factor data is statistically significant and might be resolved by the inclusion of meson exchange currents. In Fig. 2 we show the active pp and np phases in the fit with their propagated errors and compare them with the PWA [5] and the AV18 potential [7] which provided a $\chi^2/{\rm d.o.f} \lesssim 1$. Note that the $J = 1$ phases show some discrepancies at higher energies, particularly in the ϵ_1 phase, where it is about the difference between the PWA and the AV18 potential. Likewise, in Figs. 3, 4, 5, and 6 we also show a similar comparison for the pp and np Wolfenstein parameters for several LAB energies.

Finally, as the previous analyses [5–9] and the present paper show, the form of the potential is not unique providing a source of systematic errors. A step along these lines has been undertaken in Ref. [32]. Thus, the uncertainties will generally be larger than those of the purely statistical nature estimated here.

IV. CONCLUSIONS

To summarize, we have determined a high-quality proton-proton and neutron-proton interaction from a simultaneous fit to scattering data and the deuteron binding energy with $\chi^2/{\rm d.o.f.} = 1.06$. Our short range potential consists of a few δ shells for the lowest partial waves. In addition, charge-dependent electromagnetic interactions and one pion exchange are implemented. We provide error estimates on our fitting parameters. Further details will be presented elsewhere.

ACKNOWLEDGMENTS

We warmly thank Franz Gross for useful communications and providing data files. We also thank R. Schiavilla and R. Machleidt for communications. This work is partially supported by Spanish DGI (Grant No. FIS2011-24149) and Junta de Andalucía (Grant No. FQM225). R.N.P. is supported by a Mexican CONACYT grant.

[1] R. Machleidt, Adv. Nucl. Phys. **19**, 189 (1989).
[2] R. Machleidt and D. Entem, Phys. Rep. **503**, 1 (2011).
[3] W. Glöckle, *The Quantum Mechanical Few-Body Problem* (Springer-Verlag, Berlin, 1983).
[4] R. A. Arndt, W. J. Briscoe, I. I. Strakovsky, and R. L. Workman, Phys. Rev. C **76**, 025209 (2007).
[5] V. G. J. Stoks, R. A. M. Klomp, M. C. M. Rentmeester, and J. J. de Swart, Phys. Rev. C **48**, 792 (1993).
[6] V. G. J. Stoks, R. A. M. Klomp, C. P. F. Terheggen, and J. J. de Swart, Phys. Rev. C **49**, 2950 (1994).
[7] R. B. Wiringa, V. G. J. Stoks, and R. Schiavilla, Phys. Rev. C **51**, 38 (1995).
[8] R. Machleidt, Phys. Rev. C **63**, 024001 (2001).
[9] F. Gross and A. Stadler, Phys. Rev. C **78**, 014005 (2008).
[10] J. R. Taylor, *An Introduction to Error Analysis: The Study of Uncertainties in Physical Measurements* (University Science Books, Sausalito, California, 1997).
[11] C. V. D. Leun and C. Alderliesten, Nucl. Phys. A **380**, 261 (1982).
[12] I. Borbly, W. Grebler, V. Knig, P. A. Schmelzbach, and A. M. Mukhamedzhanov, Phys. Lett. B **160**, 17 (1985).
[13] N. L. Rodning and L. D. Knutson, Phys. Rev. C **41**, 898 (1990).
[14] S. Klarsfeld, J. Martorell, J. A. Oteo, M. Nishimura, and D. W. L. Sprung, Nucl. Phys. A **456**, 373 (1986).
[15] D. M. Bishop and L. M. Cheung, Phys. Rev. A **20**, 381 (1979).
[16] J. J. de Swart, C. P. F. Terheggen, and V. G. J. Stoks, arXiv:nucl-th/9509032.
[17] F. Calogero, *Variable Phase Approach to Potential Scattering* (Academic Press, New York, 1967).
[18] J. B. Aviles, Phys. Rev. C **6**, 1467 (1972).
[19] M. P. Valderrama and E. R. Arriola, Phys. Rev. C **72**, 044007 (2005).
[20] D. R. Entem, E. RuizArriola, M. PavonValderrama, and R. Machleidt, Phys. Rev. C **77**, 044006 (2008).
[21] R. Navarro Perez, J. Amaro, and E. Ruiz Arriola, Prog. Part. Nucl. Phys. **67**, 359 (2012).
[22] L. Durand, Phys. Rev. **108**, 1597 (1957).
[23] V. G. J. Stoks and J. J. De Swart, Phys. Rev. C **42**, 1235 (1990).
[24] W. H. Press, S. A. Teukolsky, W. T. Vetterling, and B. P. Flannery, *Numerical Recipes 3rd Edition: The Art of Scientific Computing* (Cambridge University Press, New York, 2007).
[25] http://nn-online.org/.
[26] http://gwdac.phys.gwu.edu/analysis/nn_analysis.html.
[27] *NN* provider, https://play.google.com/store/apps/details?id=es.ugr.amaro.nnprovider.
[28] R. T. Braun, W. Tornow, C. R. Howell, D. E. Gonzalez Trotter, C. D. Roper, F. Salinas, H. R. Setze, R. L. Walter, and G. J. Weisel, Phys. Lett. B **660**, 161 (2008).
[29] B. H. Daub, V. Henzl, M. A. Kovash, J. L. Matthews, Z. W. Miller, K. Shoniyozov, and H. Yang, Phys. Rev. C **87**, 014005 (2013).
[30] M. H. MacGregor, R. A. Arndt, and R. M. Wright, Phys. Rev. **169**, 1128 (1968).
[31] R. A. Gilman and F. Gross, J. Phys. G **28**, R37 (2002).
[32] R. Navarro Perez, J. E. Amaro, and E. Ruiz Arriola, Phys. Lett. B **724**, 138 (2013).